Study of the ECAL timing effects due to transparency using π^0 Decays from the CMS Experiment

Kai Chang
Mentor: Maria Spiropulu, Adi Bornheim, Emanuele Di Marco

Abstract

The CMS ECAL is capable measuring the energy of high energy photons with a precision of about 1% and their time of arrival in the detector with a precision of around 100 ps. The calibration of the detector *in situ* with neutral pion decays into two photons is a crucial step to achieve the energy resolution performance. To date the timing response is calibrated with generic calorimeter clusters which have the characteristics of electromagnetic interactions. One important systematic effect limiting the timing performance is the radiation induced transparency change of the crystals. This modifies the optical path of the scintillation photons in the crystals which changes the time response. In this project the measurement of the crystal transparency will be used to study this dependency an derive a correction for the timing measurement. The π^0 calibration sample and analysis framework will serve as a clean benchmark sample to test the corrections.

1 Introduction

Since the start of the Compact Muon Solenoid (CMS) experiment in 2008, trillions of proton to proton collisions have occurred at incredibly high energies on the scale of tera electron Volts (TeV). Prominent discoveries have been made in Physics with the CMS experiment, notably the Higgs Boson Particle (2012), which explained the origin of mass of subatomic particles.

With the production of so many proton-proton collisions at high energies (the most recent being 13 TeV), the detector experiences extreme radiation conditions. These intensive radiation settings have been found to damage scintillating crystals in the CMS detector over time, changing their colors and molecular structures. The damage, known as Hadronic damage and Electromagnetic damage, have the greatest effect on the most inner layer of the CMS, the Electromagnetic Calorimeter (ECAL).

Hadronic damage, caused by the hadron irradiation, is permanent on the crystal, causing extreme molecular changes. The result are physical holes in the ECAL. Electromagnetic damage on the other hand, caused by high energy photon (γ) irradiation, is temporary and its damage is recovered over a long time period. The result of an ECAL crystal going under EM damage is a loss in transparency by change in color. The transparency effect is not as significant in the barrel of the ECAL but is significant in the two endcaps (EE+, EE-). As the proton beam enters through a hole in the center of the barrel, a significant fraction of the beams will wander off course, hitting the barrel with a much higher probability than the endcap. Thus, it is reason to believe the inner ring of the endcaps suffer a significant the most change in transparency.

Now, although we see a recovery in the crystals' transparency over time from this electromagnetic radiation damage, this recovery state happens over durations on the magnitude of months. So, it is expected the transparency is non optimal (100%) during any time of our 13 TeV run, meaning our data would not be accurate.

Studies have shown the effects radiation damage have the amount of light input, making data harder to select for further analysis.

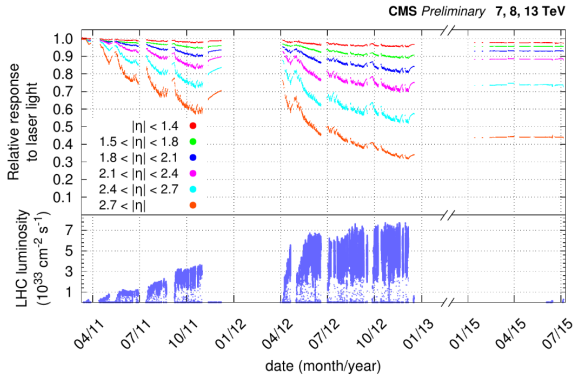

Figure 1: *Evolution of Crystal Transparency through the CMS Runs*

Thus, the CMS experiment, with Caltech leading the charge, built a Laser Monitoring System to continuously record the transparency changes in each crystal in real time. After data taking, CMS then applies a correctional gain on the RAW data, removing the transparency effect on the energies of the photon seed deposition.

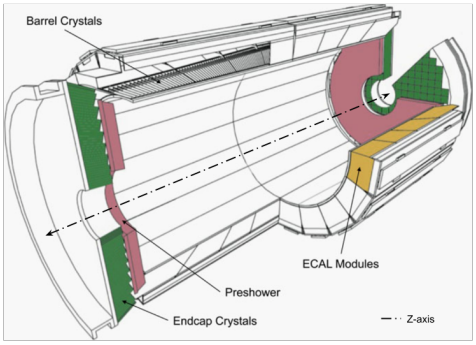

Figure 2: *ECAL, referencing z-axis beam line and split of half barrel as x,y-axis*

It's been long believed the transparency change on the ECAL crystals also plays a role in the change of the timing response. Since pions are neutral, they are not affected by the magnetic field produced in the CMS, meaning they follow a linear trajectory. Thus, we assume their time of arrival on the crystal is the same, or follows a very tight normal distribution. However, the change in transparency in the crystal is hypothesized to effect the time between when the photons from the pions are produced to when their energies are detected by the photo multiplier tube and readout signal in the backend of the scintillator crystals. This time, δ, is expected to increase due to this change in transparency. We expect that this change is most likely due to the molecular changes in the ECAL crystal, resulting in a non-optimal path for the photons to travel and interact either through compton scattering, photoelectric effect, or pair production.

Until now, there have been no direct studies on the relationship between transparency of the crystal and their timing responses at 13 TeV. We will determine the relationship by fitting the evolution of the timing response over transparency (indirectly time) using neutral pions, π^0. We choose π^0 because it is relative abundant from the collisions, they have lower energies and easier primary decay states, making them easier to pick out, and they have zero spin, unaffected by the strong magnetic field. A correction factor is produced and compared for performance, determining the significance of transparency on a crystal's timing response performance.

This is especially important in the upcoming runs and the future developments of the CMS experiment due to the increase in luminosity or ramp up of collisions in shorter time frames. With much more events added per bunching, way more uninteresting events occur in our detector, causing what is known as a pileup. As of now, we deal with pileup by parametrizing position and energy, applying what is known as a 4 dimensional cut. This yields good enough resolutions in our data and removes enough non-interesting events for our current analysis. However, down the road, with a slated increase in luminosity and shorter collision time spacing, another dimension is desired to perform better selections of events. This fifth dimension will be time. My ongoing project attempts to calibrate time such that such a selection cut is possible. The first study is in examining transparency association with timing.

2 Methods

2.1 Selection Criteria for π^0

To gather the appropriate neutral pion data for studies at 13 TeV, we took advantage of the already available data extractor program, ECALpro, and applied it to the real-time data as they were outputted. We

modified the ECALpro to extract more characteristics of interest to be used for our studies.

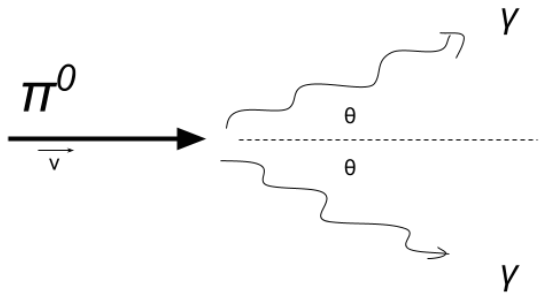

Figure 3: *Neutral Pion Decay into $\gamma\gamma$, the most common form of decay*

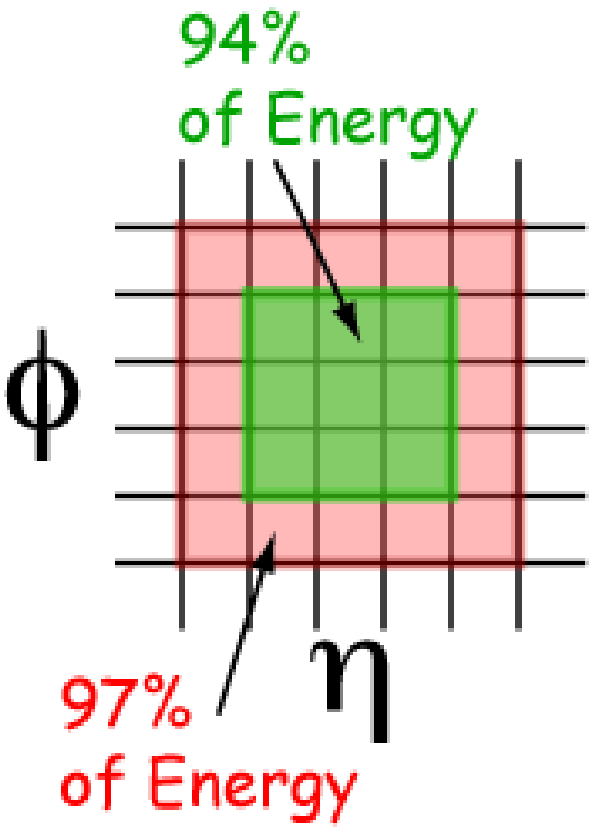

Figure 4: *Seed energy deposition distribution amongst crystals*

To maximize statistic, we lowered our cut threshold for potential pion candidates. The initial cuts were applied to different regions of the ECAL, the inner barrel, outer barrel, low eta and high eta in the endcaps (EE). This was because although they were of different positions in the calorimeter, their relative eta were the same, meaning the pions that interacted at those regions had similar properties. We applied a preliminary low and high transverse momentum cut (pT), a seed crystal cut, a 2x2 crystal matrix deposition over 3x3 matrix deposition ratio cut, a transverse momentum cut for each individual photon, and and isolation cut to determine the energy deposited in the ECAL in nearby crystals of the potential pion decay location. A secondary cut was required to eliminate bad data, or data without enough statistic. This criteria yielded sufficient data to study. In order to determine a neutral pion candidate, we took the energies of the seed deposition in a 3x3 cluster, as 94% of the energy is absorbed within this layer, and 97% within a 5x5 cluster.

In order to separate by transparency, we then binned the data by weeks or more commonly runs, depending on the time duration and data size. Binning by time was appropriate because the transparency effects are relatively identical within a time frame, and stacking the data in larger time frames allows for better resolution on our statistic.

Since the endcap has the most change in transparency from observations of previous experiments, the primary goal of this investigation and insight will be on the performance change in the endcap region. We will use the barrel data, which is generally more consistent due to the increase of statistics, as a check on our hypothesis, but the primary focus in this project is looking at the endcap region.

2.2 FAST_

In order to accomplish data acquisition and analysis, **FAST_** was developed. FAST_ extracts, fits, and arranges the data so that I would be able to ana-

lyze or investigate the findings. It's a robust package ($> 10,000$ lines of code!) automating the extraction and organization part of the data. In a more analogous term, the package would be able to do the "data taking" and "fitting" in a traditional experiment on a larger and faster scale. FAST_ was optimized for looking into many aspects and investigating all kinds of conditions in transparency and timing response; some including looking into eta regions, cluster regions, and comparing two runs with each other to conceptual challenge the hypothesis.

This package offers a minimal learning curve to those that would continue onwards with the project. Knowing that calibration for the ECAL would continue in the long run, as the CMS experiment has been slated to continue into at minimum the next decade, anyone who wished to study this further, or include these data extractions for further study in other investigations, would be able to without having to rewrite a similar code from scratch. This is collaboration at its purest, with my package as an imprint for others to use and modify as pleased. I based my FAST_ package off of a similarly existing package for extracting π^0 mass called **ECALpro**, which was developed by a group of graduate students, notably Luca Pernie (*INFN*, *IIHE*). I used his package and modified it for my package as well.

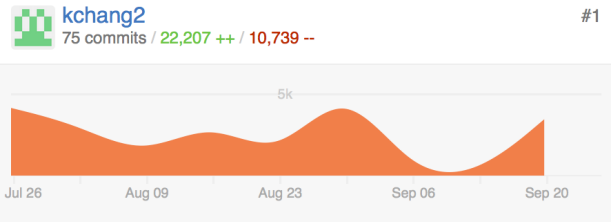

Figure 5: *Contributions to the FAST_ package*

2.3 Data Analysis

For each individual crystal's time response and transparency histograms, we applied either a gaussian fit or a simple mean calculation. The decision of which method would be used was based solely on the number of statistic we had. We applied a normal distribution because we expected there be randomness and variations with the energy deposition on the crystals. We took the mean because the numbers at low statistic in a normal distribution could be applied appropriately due to symmetry. Note we consider to take the Chebyshev polynomial background because there is no defined pattern for the background noise. We did not because there were no defined justifications for it. The only value we needed from the Gaussian fit was the mean and the uncertainty of the mean. With the instrumentation error, cosmic particles coming by, and unaligned beams, a constant background was inappropriate.

Since the laser transparency data comes in as factors of amplification from the Laser Monitoring System, a simple inverse was applied to get the relative "transparency". If no amplification was needed, the transparency factor would be 1, and relative transparency is the inverse of 1, which also yields 1.

$$y(x; A, \mu, \sigma) = Ae^{-(x-\mu)^2/2\sigma^2} \tag{1}$$

where A is the amplitude of the peak distribution, x is the time response value or transparency value, μ is the mean time response or transparency, σ is the spread of the time response distribution. Note that the amplitude is non-significant in our fit, as the number of counts is only useful in defining a distribution.

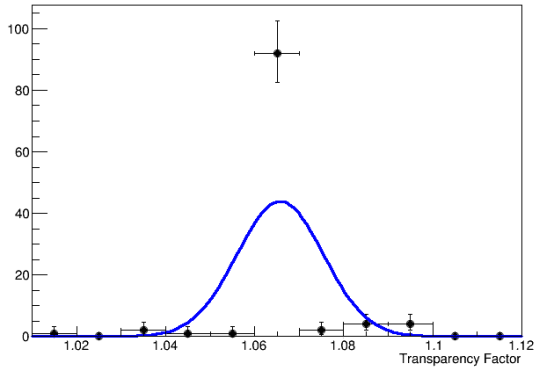

Figure 6: *Transparency Gaussian Fit, Run 2015A (EE-, 91, 30)*

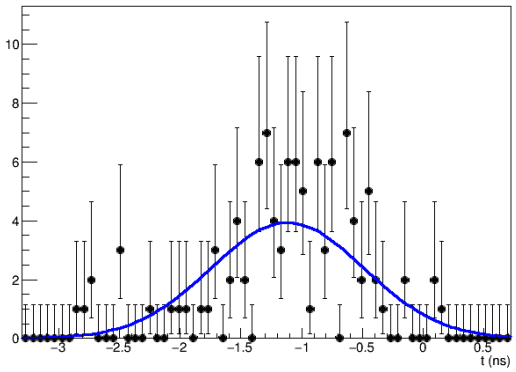

Figure 7: *Time Response Gaussian Fit, Run 2015A (EE-, 91, 30)*

$$\mu(x;n) = \frac{\sum_{i=1}^{n} x_i}{n} \tag{2}$$

where x_i is a time response value, n is the number of data points per crystal, the sample size.

$$\sigma(x;N,\mu) = \sqrt{\frac{1}{N-1}\sum_{i=1}^{N}(x_i-\mu)^2} \tag{3}$$

where x is the instant time response data point, N is sample size, and μ is the sample mean.

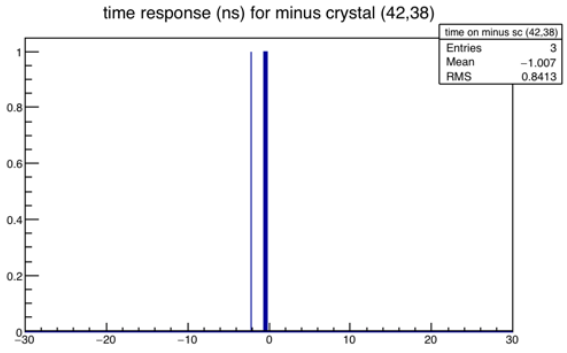

Figure 8: *Time Response Mean Fit becomes more appropriate with statistic = 3, Run 2015A (EE-, 42, 38)*

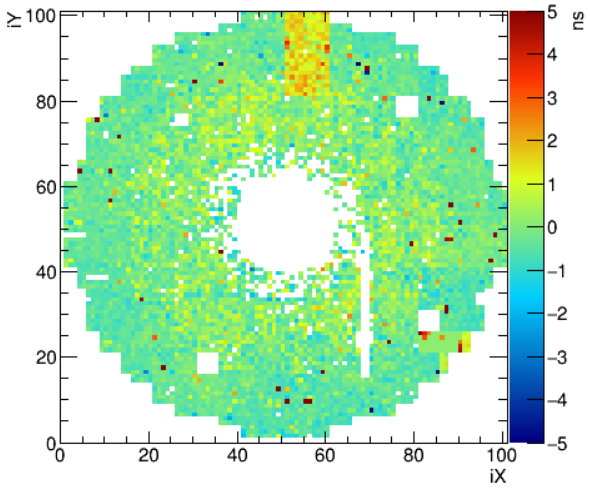

Figure 9: *Time Response Map, Run 2015A EE+*

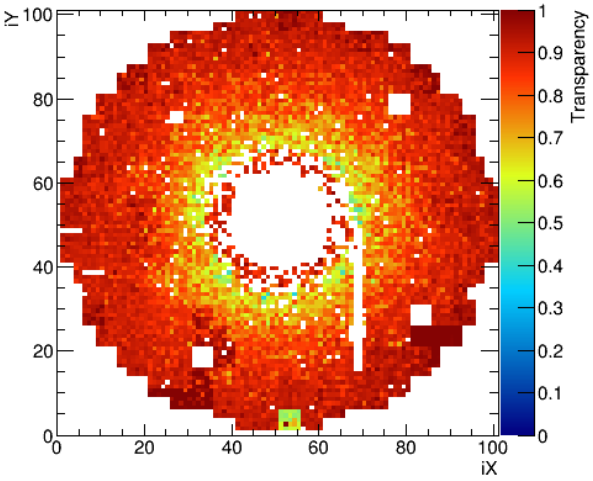

Figure 10: *Transparency Crystals Map, Run 2015A EE+. Note the lack of statistic in the inner region (highest eta) → possible explanation for such endcap transparency*

From there, a 2D map of the ECAL was drawn and plotted with the found time response, laser transparency,

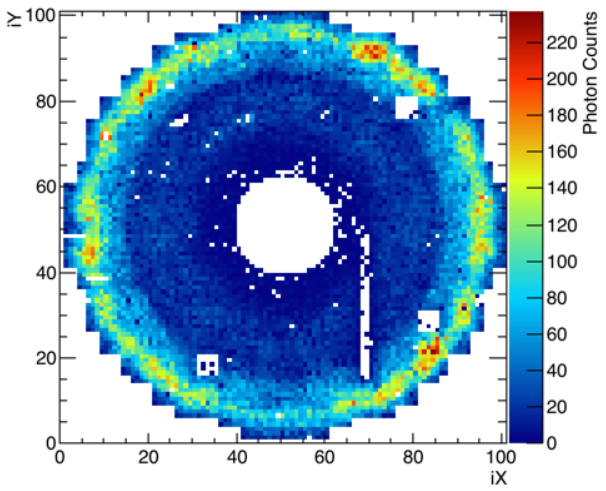

Figure 11: *Seed Density Map, Run 2015A EE+. Note the white spots within the detector → the crystals either lack statistic or instrument dead.*

and statistics. Scales were matched to show any changes in the time response, or transparency, with respect to color.

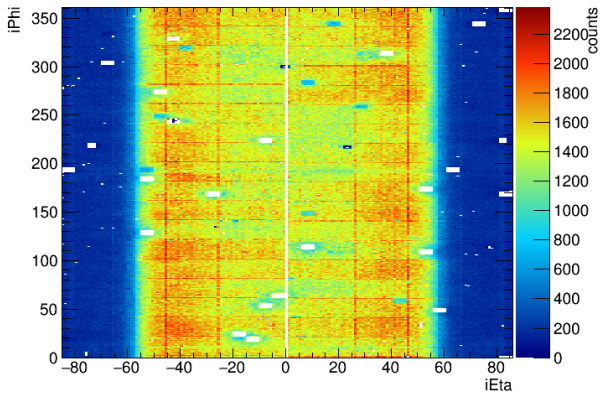

Figure 12: *Seed Density Map, Run 2015A EB. Note the significant statistic increase in the barrel.*

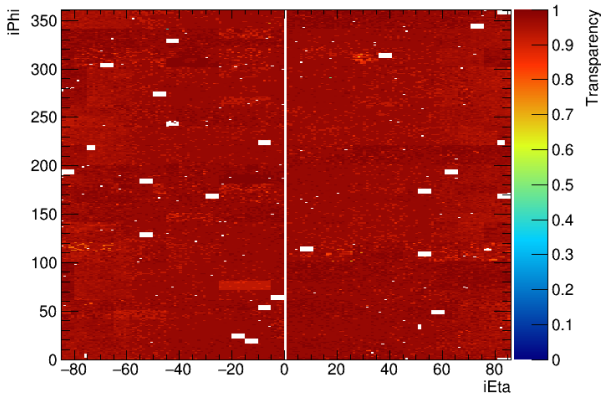

Figure 13: *Transparency Map, Run 2015A EB. Note the similarities on both ends of the barrel.*

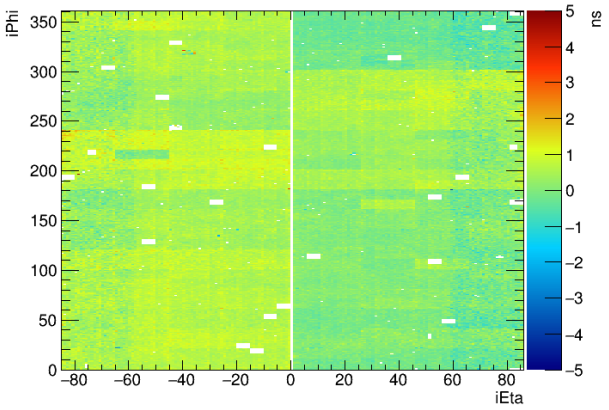

Figure 14: *Time Response Map, Run 2015A EB. Note the difference in timing response from the left side of the barrel and the right side of the barrel.*

The barrel is closer in eta to the vertex of the collision (along the z=axis, at iEta = 0 or eta = 0), meaning there is more statistic and the fits are more likely Gaussian. However, note that from the **figure**, we note that the change in time response and laser transparency does not have a large effect or difference.

Seeing the barrel figures, we justify the individual fits for each individual crystal, and the lack of grouping of all data points. From the transparency map, we see no significant difference between the left side of the barrel (iEta < 0) and the right side (iEta > 0). However, when one observes the time response on these crystals, we notice a significant color change, signaling a time response change, between the left and right half. This justifies the fact that one cannot

combine all crystal data into 1 plot or correction for maximum statistic. Each crystal is relative to itself and it's surrounding neighbors.

2.3.1 Preliminary Results

We investigate the difference in a 2D map. The results are comforting, as they are suggestive of our hypothesis.

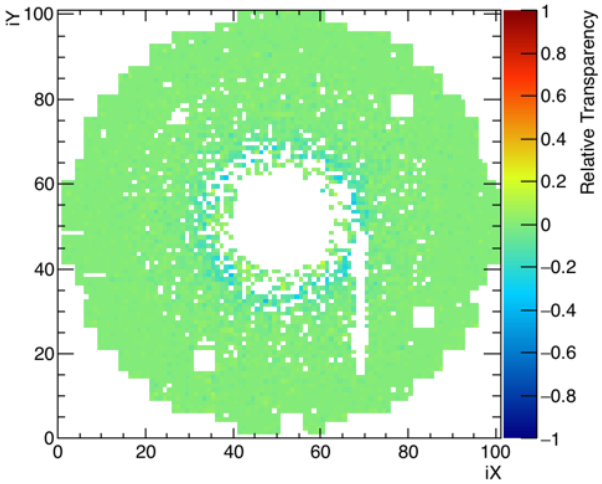

Figure 15: *Transparency Difference, 2015A - 2015B EE+*

For the most part, the transparency between 2015A and 2015B did not show any significant change. This could be because the CMS detector was shut down due to technical and instrumental issues in between these runs, and the 2015B Run was delayed for a few weeks. A few weeks could be enough time to allow the crystals to recover the transparency loss from 2015A. In addition, 2015A and 2015B had relatively small statistic, meaning that they had experienced the least damaging effects from the proton beams. This likely lessens the transparency changes as well.

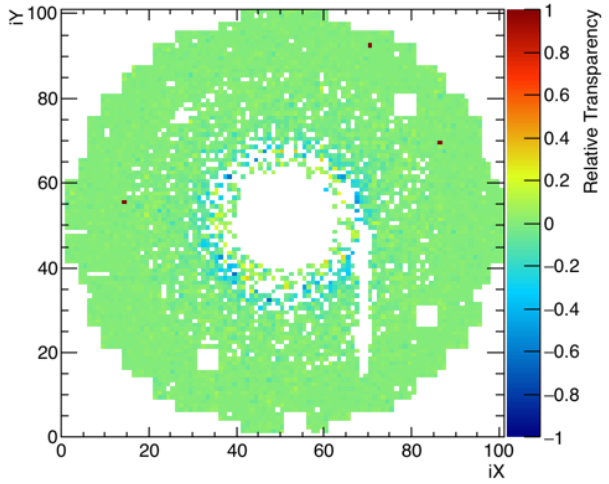

Figure 16: *Transparency Difference, 2015A - 2015C EE+*

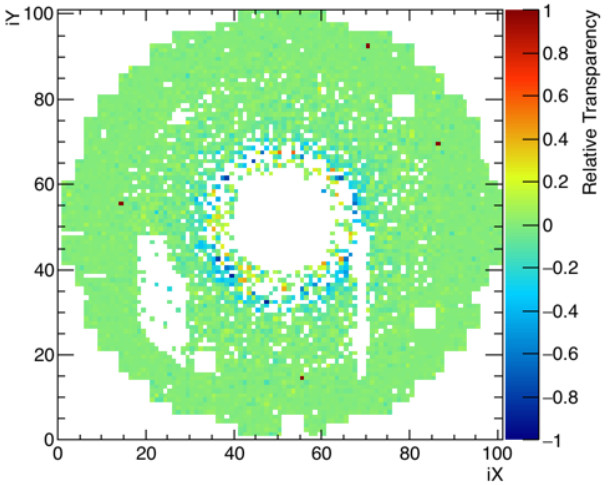

Figure 17: *Transparency Difference, 2015A - 2015D EE+*

There is a clear sign of larger transparency changes developing with more modern runs, specifically in the inner ring of the endcaps. The change becomes more negatively shifted (meaning the transparency decreases), and beings to spread outwards from the beam line axis (center).

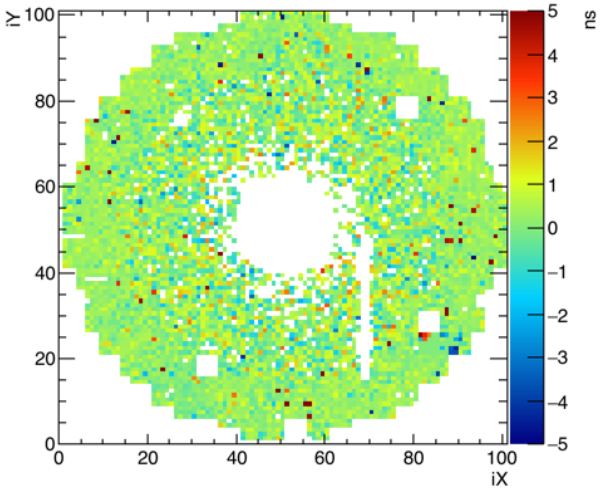

Figure 18: *Time Response Difference, 2015A - 2015C EE+*

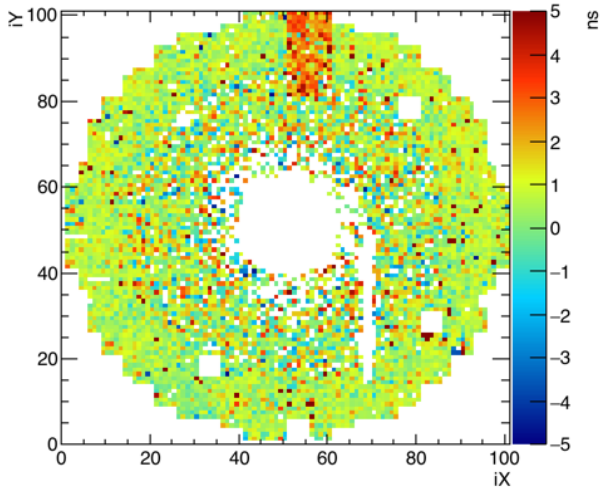

Figure 19: *Response Difference, 2015A - 2015C EE+*

Along with the trend of a transparency change in the negative direction relative to the first run of 2015, the time response also shows a direct change with respect to runs. Although this is much harder to determine from the graph, we notice there are more changes, whether positive or negative, in the time response. The difference is much more obvious, and this happens to be more than just the visible transparency ring changes in the inner circle. The time response reaches outward and seems to affect the entire endcap.

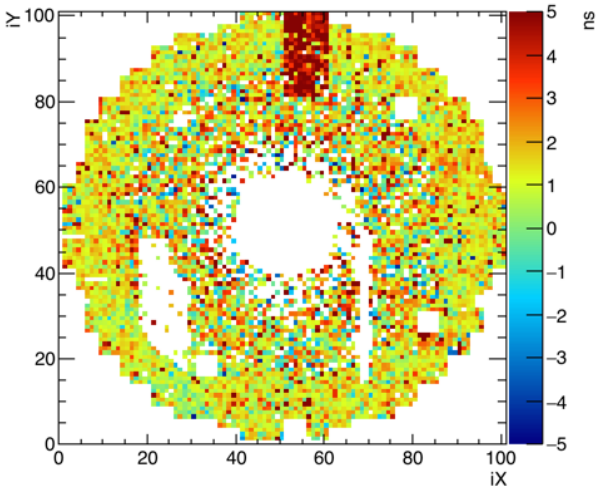

Figure 20: *Response Difference, 2015A - 2015C EE+*

2.3.2 Re-Clustering

We also clustered our crystals in 2x2 groupings specifically in the endcap, to cover crystals with insufficient statistic.

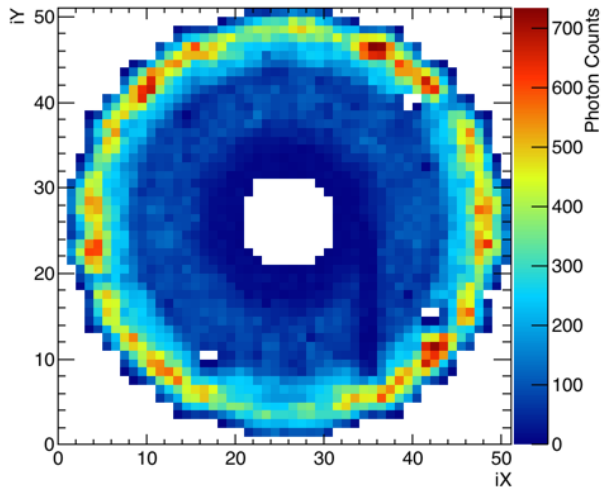

Figure 21: *Seed Density Cluster Map, Run 2015A EE+*

Although we want to investigate each crystal's own time response and transparency, from the relative frequency of energy deposition and radiation intensity in neighboring ECAL crystals, we expected neighboring crystals to have similar transparencies, thus having similar time response effects. Thus, with similar probabilities of photon deposition from the

decay state of $\pi^0 \rightarrow \gamma\gamma$ ($98.823 \pm 0.0034\%$) and having mean life of $8.30 \pm 0.19 \times 10^{-}17$s, immediately neighboring crystals are assumed to be almost identical in transparency and time response, given the initial condition that the crystals' absolute transparency were similar. With each crystal distance away, this similarity becomes increasingly less.

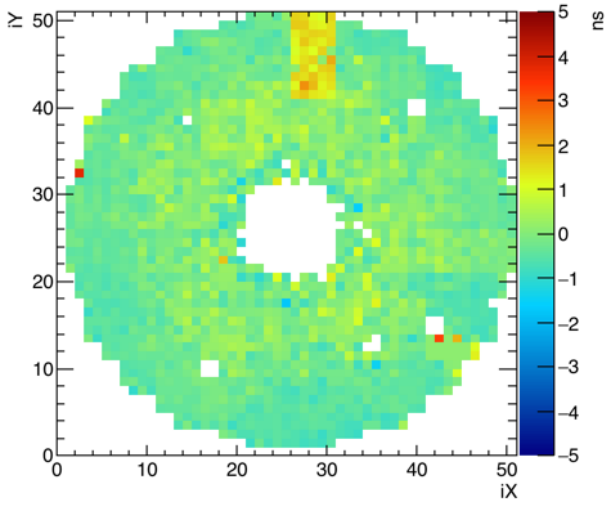

Figure 22: *Time Response Clustered Map, Run 2015A EE+*

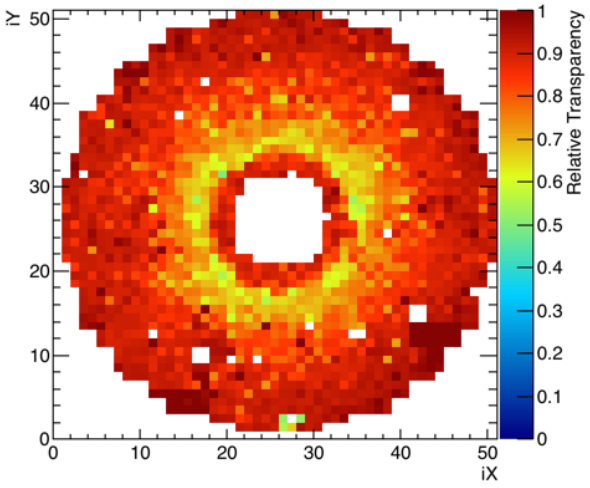

Figure 23: *Relative Transparency Clustered Map, Run 2015A EE+*

With the 2x2 groupings, we get a larger statistic per crystal, making the gaussian fit more frequent. Using eta rings was appropriate as similar eta crystals experience the same frequencies, and thus are expected to have relatively close time response and transparency values.

Now reapplying our difference plots on the clusters, the preliminary results become much more clear.

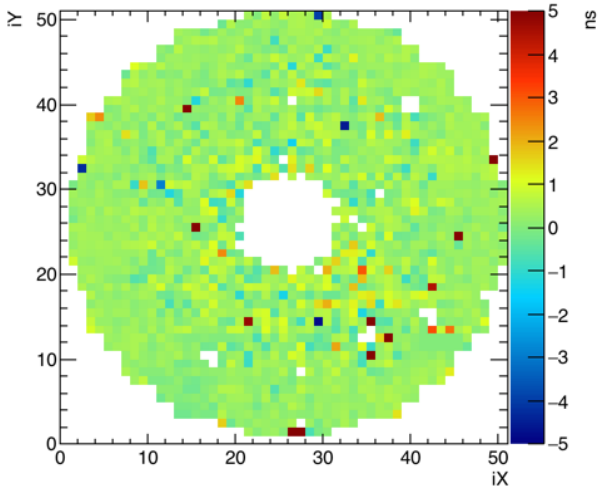

Figure 24: *Clustered Time Response Difference, 2015A - 2015B EE+*

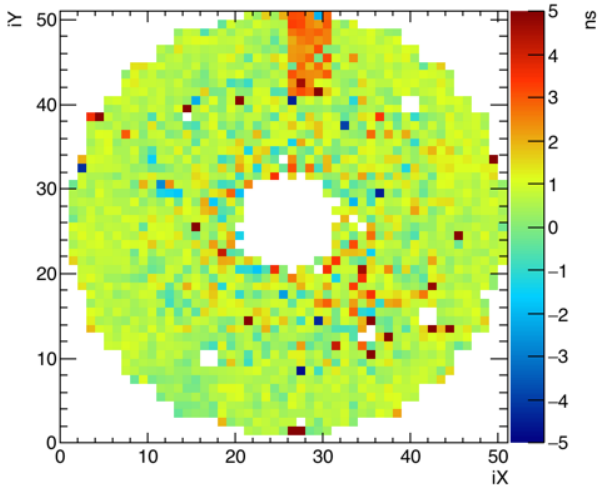

Figure 25: *Response Difference, 2015A - 2015C EE+*

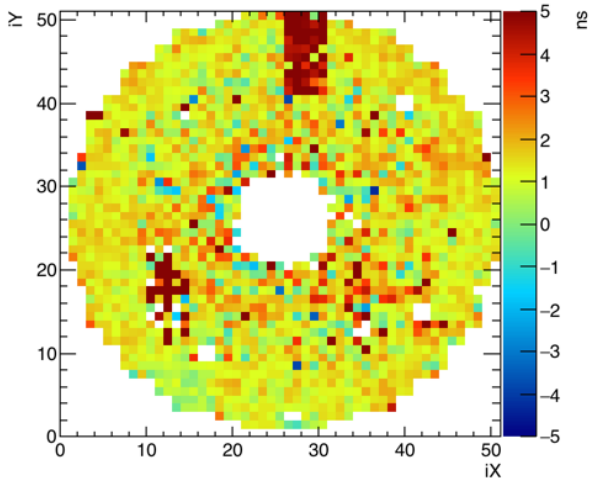

Figure 26: *Response Difference, 2015A - 2015D EE+*

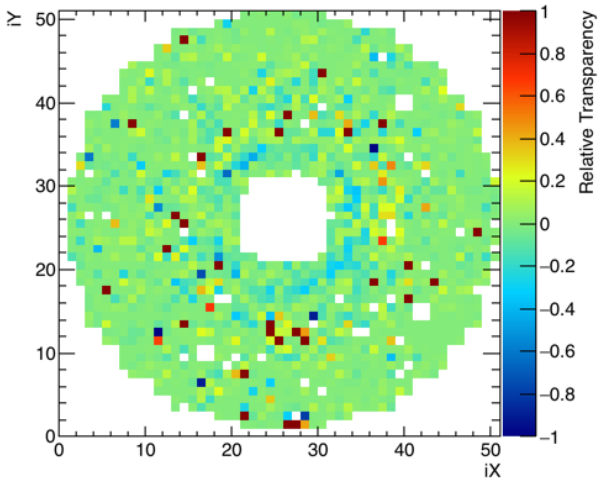

Figure 28: *Transparency Difference, 2015A - 2015C EE+*

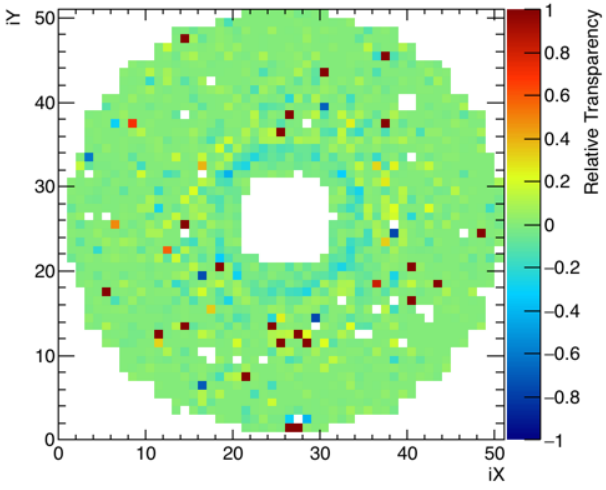

Figure 27: *Clustered Transparency Difference, 2015A - 2015B EE+*

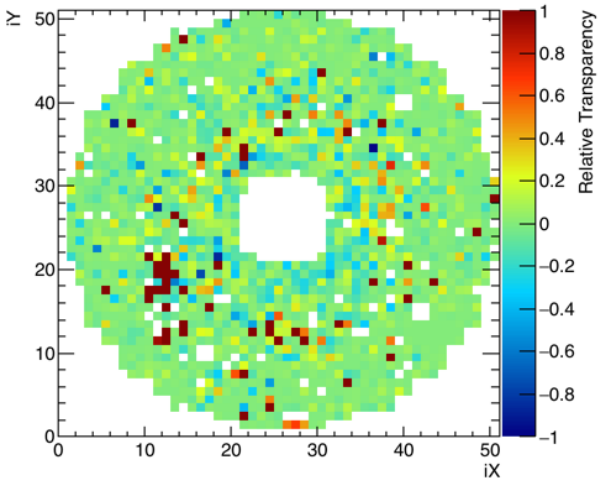

Figure 29: *Transparency Difference, 2015A - 2015D EE+*

We notice a lot easier the evolution of the transparency over time as well as the timing response. Since we clustered our crystals, we have reduced significant uncertainty and "noise" in our model by increasing the statistic by almost 4 fold. The transparency and time response difference is **consistently** larger nearer the beam line axis ($\hat{z}$), but we notice the change in time response difference is more scattered throughout the entire endcap. The transparency is also scattered, but to less of a degree.

2.3.3 Fitting the appropriate model

A series of fits were applied to each crystal to determine the true relationship between transparency and time response. The most hypothesized fit was the linear fit. We applied the following fit:

$$r = At + C \tag{4}$$

where r is the time response and t is the relative transparency, using ROOT and Python again (see Appendix A).

When plotting the transparencies and time responses, we assumed the transparencies would decrease uniformly over time. Although the ECAL crystal transparencies decrease in a non-uniform fashion in real time because of the on and off procedure for data taking in the LHC, the general trend is a linear decrease in fashion, as seen in figure one. Thus, each of the data points collected were within the same conditions. There was a significant issue with the helium superconductor during the first six weeks of my stay at CERN, so the crystals experienced larger than normal recoveries, and non-uniform data taking.

We also noted that in order to maximize our data points, we forgo the individual crystal fitting in the endcap region and did a fit with clusters. This is because in the cluster region, we get more statistic and meaning a higher chance of being able to extract an accurate transparency and time response. The barrel region had enough statistic to do individual crystal fits.

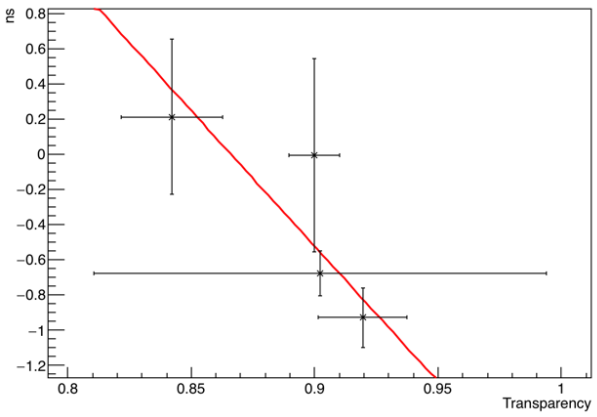

Figure 30: *time response vs. transparency, EE+ (20,30)*

$$r = -15.453t + 13.384 \tag{5}$$

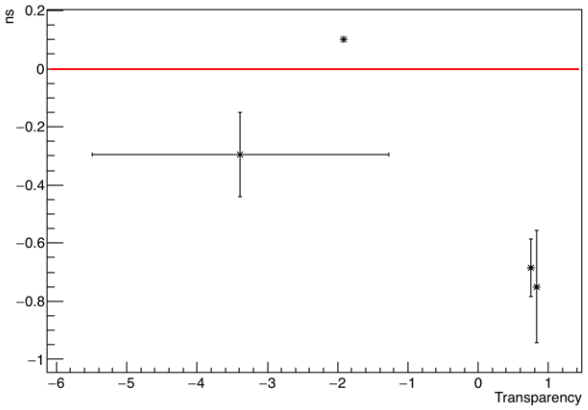

Figure 31: *time response vs. transparency, EE+ (40,20)*

$$r = 0t + 0 \tag{6}$$

You will see that in this one, we get 0 slope and 0 constant. This is because the uncertainty in the value is 0.0059 for the constant and $2.148e-14$ for the slope.

Note that we saw a high frequency of large error bars in many of our data points, and again, this can only be attributed to the fact that our statistic of pi^0 were small versus the spread of the photon energies deposition in the crystal. The high error association with our data points along with the relative spread of our data points (and inconsistency) again suggests that our binning method was not enough to produce significant enough statistics. Furthermore,

3 Results/Discussion

The linear fits we applied from the 4 data runs showed a relatively significant association between the time response and the laser transparency. As the time response increases, we see the transparency decreases. This seemed to match our predicted hypothesis. The barrel linear fits were far better in associating the two parameters than the endcap. This is due to the significantly larger statistic of pi^0 decays in the barrel region. However, what we found was that with our current clustering algorithm, we did not have enough of a statistic to apply good fits.

with our fit in the endcap having a maximum of four data points, and having 2 degrees of freedom, our fits were definitely not optimal. Now, these are 2 randomly selected fits out of > 65000 crystals in the ECAL, so this is a general sample of what the fits would most look like.

With more data coming in as runs continue in the CMS detector and the LHC, this fit will become more significant to look at, but as of now, the correction we derived should be taken with caution.
This will allow future data analysis to recalibrate the ECAL crystal using the time response correction factor based purely on transparency. Now, we are cautious about our linear fits because they do not have a significant number of data points, but the uncertainty in our fits and the accuracy of our predicted relationship will increase with more updated runs.

We notice negative time response, which is very interesting, as we expected the original hit to be 0 ns. Thus, this could be from prior hits that just haven't dissipated before the next hit came in, or most likely from the instrumentation or time calculation from the CMS detector and data analysis framework. The approach in which CMS calculates time comes from the time integration of the energy buildup (charge) in a capacitor. Thus, the construction to obtain the time interval gives us negative time periods.

We also tried to split the runs into multiple data points, but this proved only to be successful in the barrel due to the number of pions that deposited into the barrel (low eta). The endcap was difficult to acquire enough statistic with clustering, so no split was done. The pion decay detection happens at low rates, making this calibration long and time dependent.

4 Conclusions (Future Work)

The study of $pi^0 \rightarrow \gamma\gamma$ decays in the CMS detector have shown some association between the time response of the ECAL crystals and the transparency of these ECAL crystals. Although there is some association, we cannot define an absolute relationship due to the statistic in our experiment. We cannot conclude any information about the relationship between transparency and timing response in the ECAL crystals due to our lack of statistics. Our findings were inconclusive.

There is still a lot of work to be done with the ECAL calibration. More data is needed to make a better and more precise fit. Though some of the fits have been good with smaller error bars, the lack of consistent data points due to the spread and the distribution of energy and time response from the interaction paths between the crystal and the photon makes our fits not sufficient enough to be absolute. There is a need to introduce new binning methods to optimize the current data we have now. Further analysis is needed to bin the data for a better study.

Because transparency changes the scattering path of the photons that deposit their energies into the crystal (or pass through), more studies need to be done or more data needs to be taken to reduce the uncertainty in the transparency and time response from the spread of photon deposition interaction. So, until more data is given out, our fit is relatively inaccurate and not sufficient to apply a correction to see impact on performance in heavily changed areas in the ECAL.

Because transparency changes in different regions of the ECAL at different rates, it is interesting to view the symmetry in parts of the ECAL in terms of time response and transparency. So far, it appears as if the change is not symmetric, as some sides are more affected than others. The change of time response and transparency is much smaller in variation from the symmetric sides (left side of the barrel vs right side of the barrel and EE+ vs EE-) than the absolute time response and transparency. It is noted that they began in 2015 with different overall values. This could be due to the different factories where the crystals were grown (China and Russia). It would be interesting to do studies on the efficiencies of these crystals on time response from their original plantation. As for now, the linear fit

$$r = At + C \tag{7}$$

seems promising, but the results are not precise enough to compare performance difference.

There will need to be further studies and examinations as future runs come in. In addition, additional forms of clustering will be needed in order to increase statistic in our current data to reduce variation and error bars. Furthermore, there will need to be a new way of applying fits to the laser calibration data. In assuming that the laser calibration was precise, a mean fit would seem more relevant than a gaussian fit. These are ongoing works that will need to be accomplished by those working in the ECAL calibration team, and me, but the preliminary results so far seem promising. At 13 TeV and with high luminosity, high number and rate of collision, the transparency change between runs are larger than ever, and the time response are showing so.

Acknowledgements

Of the many people who deserve thanks, some are particularly prominent, such as my CERN supervisor Adolf Bornheim, my Caltech supervisor and faculty sponsor who without I would not have been given this unique opportunity, Professor Maria Spiropulu, the graduate students in the Caltech-CMS group Javier Duarte and Dustin Anderson, both of whom have assisted me in my weekly programming challenges, graduate students of other universities participating in the CMS experiment, Luca Pernie (IIHE) and Rafael Teixeira De Lima (Northeastern University), who without their expertise and their involvement in similar projects, I would not have been able to make any results you see here today, the MoCa (the Monitoring and Calibration) group for their knowledge and progress updates to increase my breadth and understanding of my project, my fellow undergraduate researcher Benjamin Bartlett, whose expertise in Python helped me run my program (significantly) more efficiently, the rest of the CMS Group at Caltech who were very supportive and offered meaningful activities while I was stationed in Geneva, and many many more...

Appendix A: Linear Fits

Complete Data EE+ (20,30)

t	σA	r	σr
0.21263812	0.84212538	0.44247896	0.02065823
−0.00426702	0.89988109	0.55018094	0.01020999
−0.67767322	0.90201329	0.13024733	0.0916754
−0.92936955	0.91947402	0.16914372	0.01806773

Table 1: A table of the necessary data used for a linear fit, specifically for the EE+ (20,30) crystal

Complete Data EE+ (40,20)

t	σA	r	σr
−0.74952016	0.82961161	0.19183338	$7.90324552e-03$
−0.68563266	0.75040263	0.09859445	$9.75736997e-03$
−0.29585847	−3.38390904	0.1461056	$2.11550572e+00$
0.1	−1.90914321	0.	$3.05448136e-04$

Table 2: A table of the necessary data used for a linear fit, specifically for the EE+ (40,20) crystal

Complete Data EE+ (20,30)

t	σA	r	σr
0.37708807	0.94612284	0.13350955	$7.38823155e-09$
0.23987305	0.94612284	0.12509698	$7.61198375e-09$
0.4632062	0.94612284	0.21620248	$5.51739060e-09$
0.18295307	0.94612284	0.07785558	$7.16573896e-09$
0.12790688	0.94612284	0.10695777	$7.27478854e-09$

Table 3: A table of the necessary data used for a linear fit, specifically for the EB (20,30) crystal

Complete Data EE+ (20,30)

t	σA	r	σr
0.69394487	0.97500001	0.05079955	$3.25185212e-10$
0.68151384	0.97501306	0.04009994	$1.48379735e-07$
0.09179465	0.95675524	0.12372664	$6.59191938e-09$
0.27104522	0.97501268	0.03074521	$8.41686454e-09$
0.42910935	0.97499894	0.02935204	$7.75879805e-10$

Table 4: A table of the necessary data used for a linear fit, specifically for the EB (40,20) crystal

time response (r) v. transparency (t) Fit, EE+

x	y	A	σA	C	σC
20	30	13.3845	-15.4532	7.3529	8.1108
40	20	0.0	0.0	0.00058736	$2.1475e-14$

Table 5: Table of linear fit results, specifically for the EE+ crystals mentioned prior

time response (r) v. transparency (t) Fit, EB

x	y	A	σA	C	σC
20	30	0.12497	0.1321	0.90378	0.9552
40	20	-19.8812	20.8766	6.6946	6.8699

Table 6: Table of linear fit results, specifically for the EB crystals mentioned prior

Appendix B: All Necessary Plots

Photon Seed Density, ECAL → number of photons that interact with the ECAL

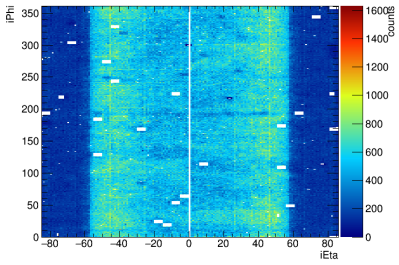

Figure 32: *ECAL Barrel, 2015B_1*

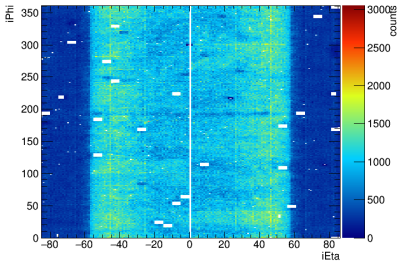

Figure 35: *ECAL Barrel, 2015B_2*

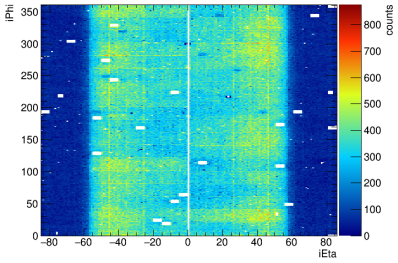

Figure 38: *ECAL Barrel, 2015C_1*

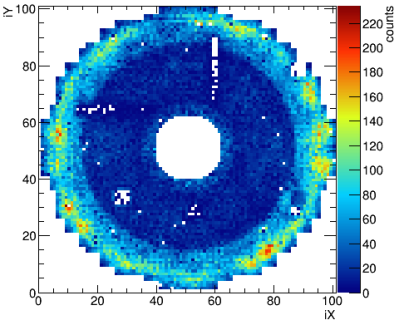

Figure 33: *ECAL EE-, 2015B*

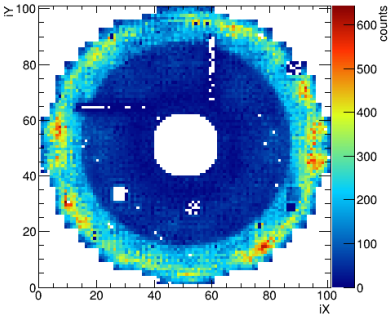

Figure 36: *ECAL EE-, 2015D*

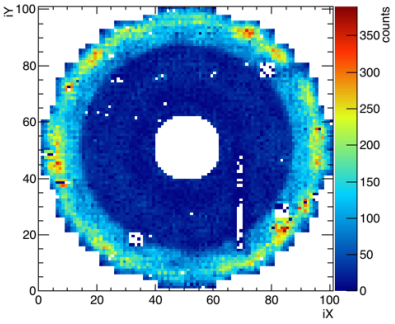

Figure 39: *ECAL EE+, 2015C*

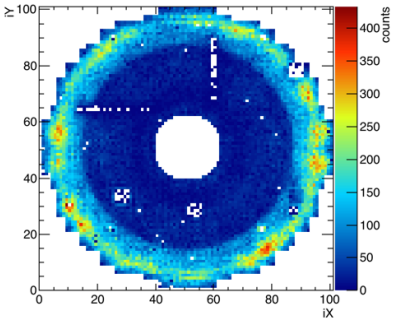

Figure 34: *ECAL EE-, 2015C*

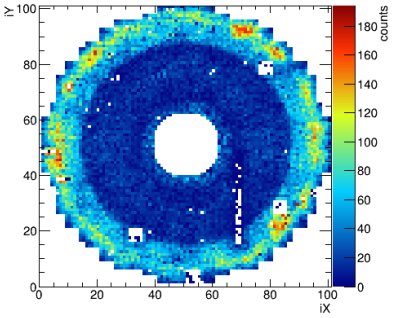

Figure 37: *ECAL EE+, 2015B*

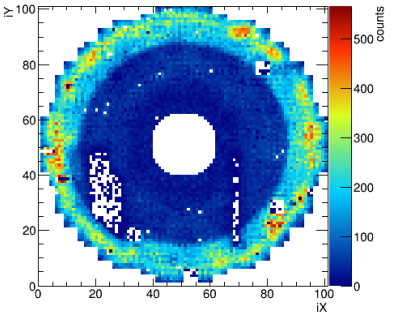

Figure 40: *ECAL EE+, 2015D*

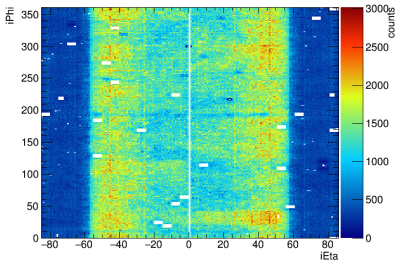

Figure 41: *ECAL Barrel, 2015C_2*

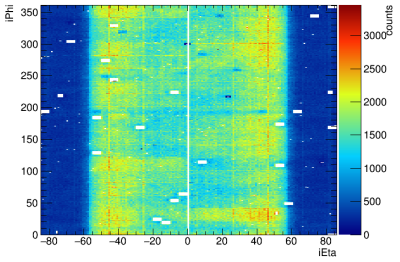

Figure 42: *ECAL Barrel, 2015C_3*

Time Response, ECAL → time of arrival of photon to deposition crystal after collision. Note collision time is zero.

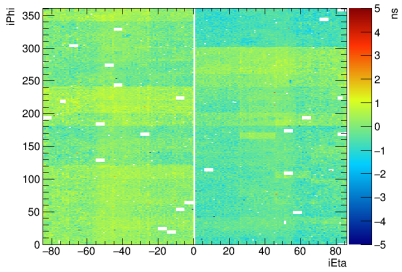

Figure 43: *ECAL Barrel, 2015B_1*

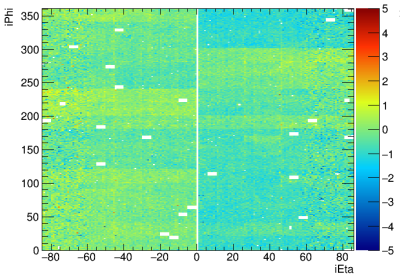

Figure 46: *ECAL Barrel, 2015C_3*

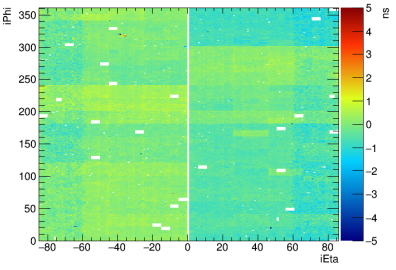

Figure 49: *ECAL Barrel, 2015C_3*

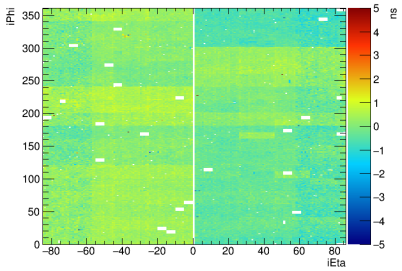

Figure 44: *ECAL Barrel, 2015B_2*

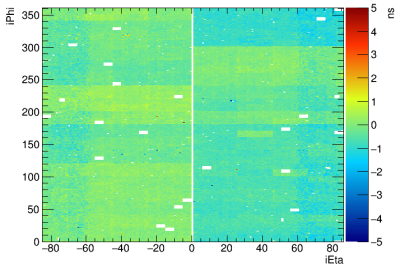

Figure 47: *ECAL Barrel, 2015C_2*

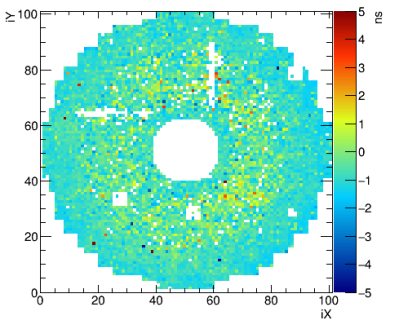

Figure 45: *ECAL EE-, 2015B*

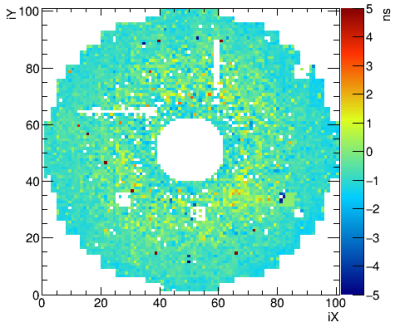

Figure 48: *ECAL EE-, 2015C*

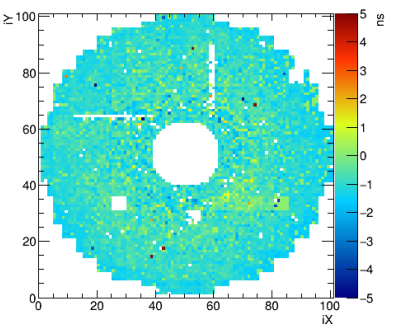

Figure 50: *ECAL EE-, 2015D*

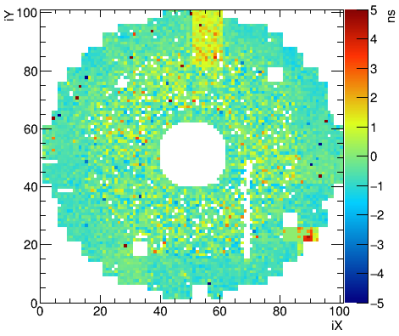

Figure 51: *ECAL EE+, 2015B*

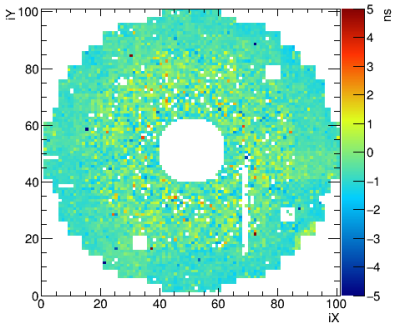

Figure 52: *ECAL EE+, 2015C*

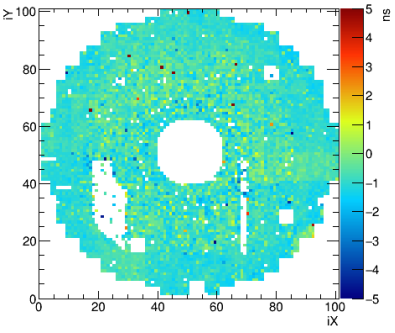

Figure 53: *ECAL EE+, 2015D*

Laser Transparency, ECAL → transparency of the crystal (relative) from a scale of 0 to 1. 1 means perfectly clear, and zero suggests no light penetration.

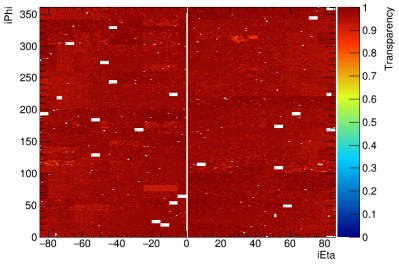

Figure 54: *ECAL EB, 2015B_1*

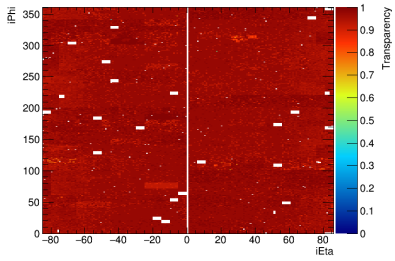

Figure 57: *ECAL EB, 2015C_2*

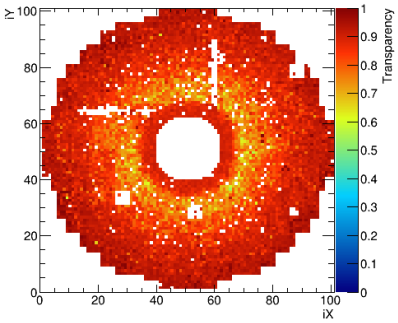

Figure 59: *ECAL EE-, 2015B*

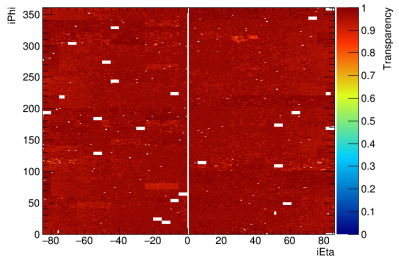

Figure 55: *ECAL EB, 2015B_2*

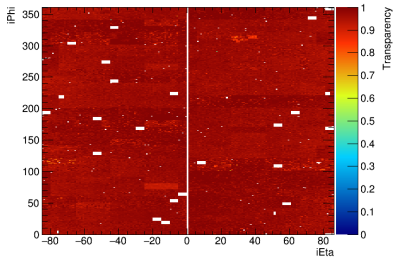

Figure 56: *ECAL EB, 2015C_1*

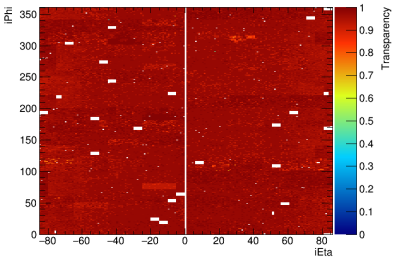

Figure 58: *ECAL EB, 2015C_3*

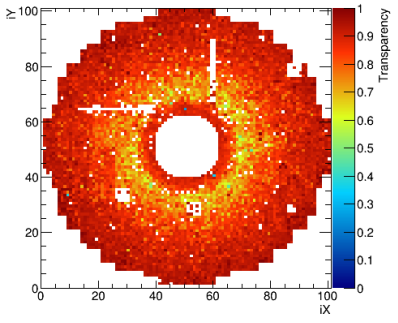

Figure 60: *ECAL EE-, 2015C*

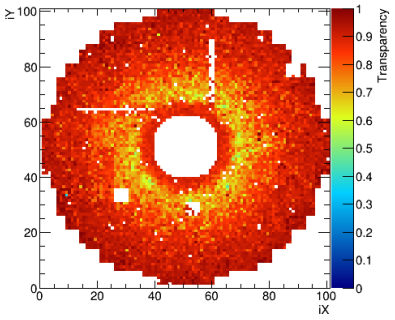

Figure 61: *ECAL EE-, 2015D*

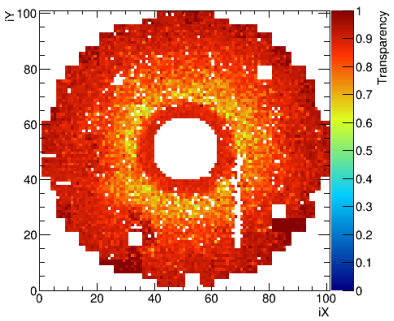

Figure 62: *ECAL EE+, 2015B*

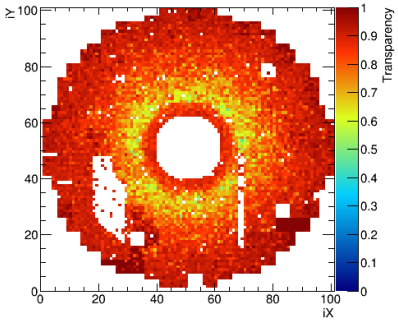

Figure 64: *ECAL EE+, 2015D*

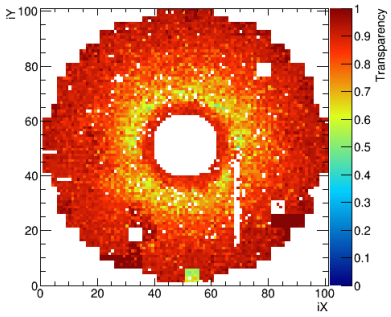

Figure 63: *ECAL EE+, 2015C*

Time response and crystal transparency difference between runs in the endcap region

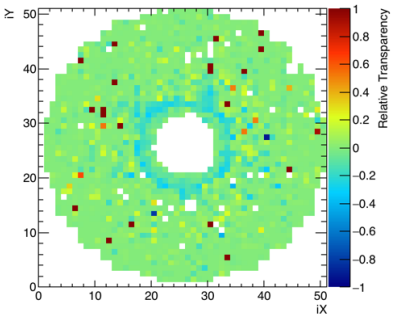

Figure 65: *Transparency Difference, 2015A - 2015B EE-*

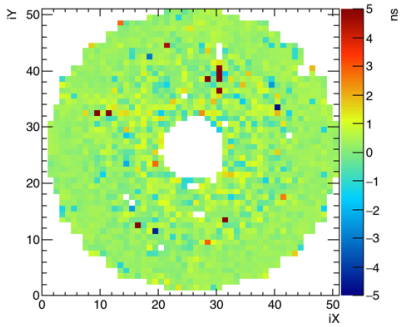

Figure 66: *Response Difference, 2015A - 2015B EE-*

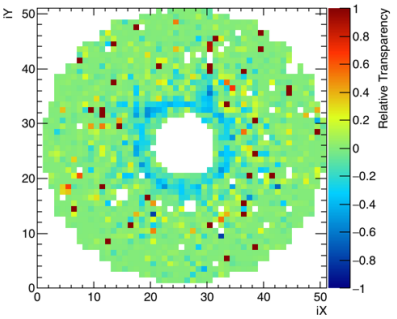

Figure 67: *Clustered Transparency Difference, 2015A - 2015C EE-*

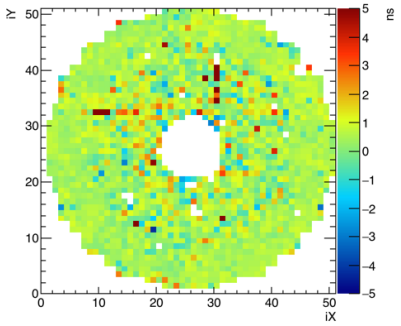

Figure 68: *Response Difference, 2015A - 2015C EE-*

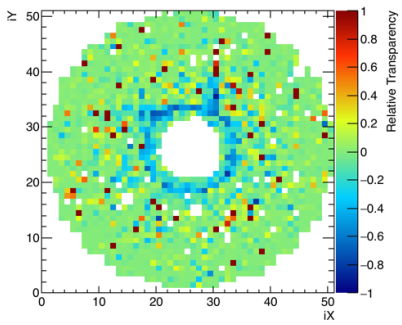

Figure 69: *Clustered Transparency Difference, 2015A - 2015D EE-*

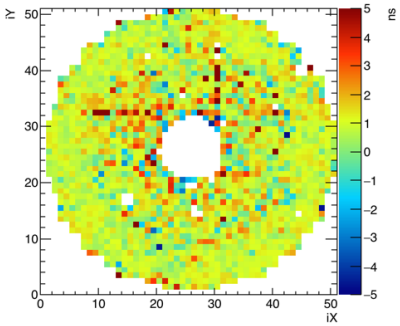

Figure 70: *Response Difference, 2015A - 2015Ds EE-*

References

Anfrevilleb M. et al. Laser monitoring system for the CMS lead tungstate crystal calorimeter. Nuclear Instruments and Methods in Physics Research Section A: Accelerators, Spectrometers, Detectors and Associated Equipment. 2006;594(2):292-320.

Bornheim A. et al. Energy Calibration and resolution of the CMS electromagnetic calorimeter in pp collisions at $\sqrt{}$ s = 7 TeV.

Bornheim A. The CMS ECAL Laser Monitoring System. Nuclear Physics B - Proceedings Supplements. 2006;197(1):219-223.

Caminada, L. (2012). Study of the Inclusive Beauty Production at CMS and Construction and Commissioning of the CMS Pixel Barrel Detector.

Evans L. Search for Radiation Induced Transparency Change in the CMS ECAL. 2010.

Timciuc V. Database usage in the CMS ECAL Laser Monitoring System.

Twiki.cern.ch. EcalDPGResultsCMSDP2013007 CMSPublic TWiki. 2015. Available at: `https://twiki.cern.ch/twiki/bin/view/CMSPublic/EcalDPGResultsCMSDP2013007`.

Yang Y. Inter-Calibration of the CMS Electromagnetic Calorimeter with $\pi^0(\eta) \to \gamma\gamma$. 2011.

Zhu K. et al. A Diode-Pumped DP2-447 Blue Laser for Monitoring CMS Lead Tungstate Crystal Calorimeter at the LHC. In: IEEE Nuclear Science Symposium, Medical Imaging Conference And RTDS Workshop. CERN; 2012.